Supporting Information Contents

A Derivation of Conditions for Achieving Different Logic Responses

In this section we derive the conditions necessary for an MWC molecule modulated by two ligands (with one binding site for each ligand) to exhibit the behavior of various logic gates shown in Figure 1. In addition to the three logic gates shown in Figure 1, we will also discuss the three complimentary gates NAND, NOR, and XNOR depicted in Figure S1.

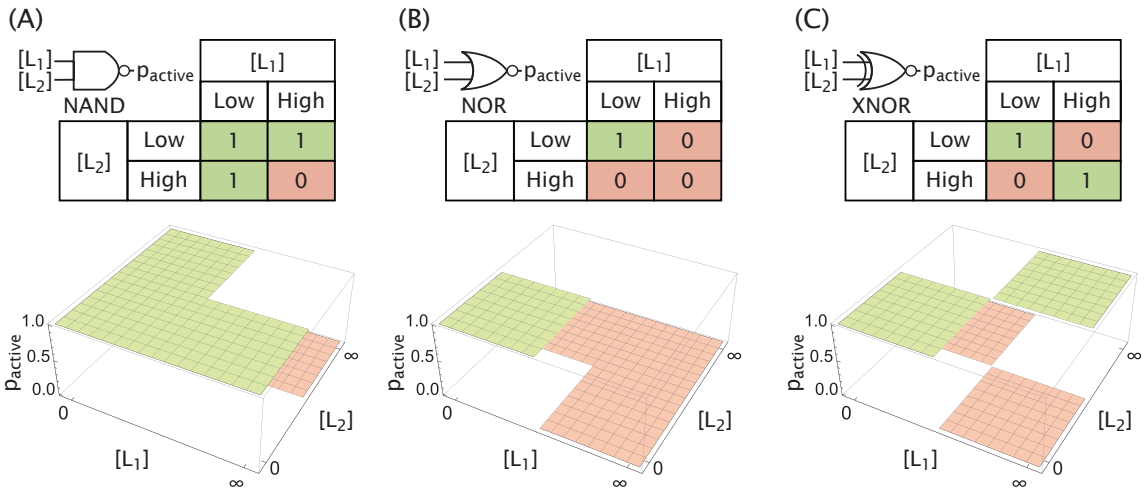

Figure S1. Additional logic gates as molecular responses. The (A) NAND, (B) NOR, and (C) XNOR gates are the compliments of the AND, OR, and XOR gates, respectively, shown in Figure 1.

To simplify our notation, we define the value of p_{active} from eq 1 in the following limits,

$$p_{0,0} = p_{active}([L_1] \to 0, [L_2] \to 0) = \frac{1}{1 + e^{-\beta \Delta \varepsilon_{AI}}}, \tag{S1}$$

$$p_{\infty,0} = p_{active}([L_1] \to \infty, [L_2] \to 0) = \frac{1}{1 + \gamma_1 e^{-\beta \Delta \varepsilon_{AI}}}, \tag{S2}$$

$$p_{0,\infty} = p_{active}([L_1] \to 0, [L_2] \to \infty) = \frac{1}{1 + \gamma_2 e^{-\beta \Delta \varepsilon_{AI}}}, \tag{S3}$$

$$p_{\infty,\infty} = p_{active}([L_1] \to \infty, [L_2] \to \infty) = \frac{1}{1 + \gamma_1 \gamma_2 e^{-\beta \Delta \varepsilon_{AI}}}, \tag{S4}$$

where $\gamma_i = \frac{K_{A,i}}{K_{I,i}}$ is the ratio of the dissociation constants between the i^{th} ligand and the protein in the active and inactive states. From the ideal logic gate behaviors visualized in Figure 1 and Figure S1, we can then deduce the desired constraints that model parameters need to meet for an effective realization of each gate.

A.1 AND Gate

Starting from the AND gate, we require $p_{0,0} \approx 0$, $p_{0,\infty} \approx 0$, $p_{\infty,0} \approx 0$ and $p_{\infty,\infty} \approx 1$, which yields the following conditions:

$$e^{-\beta\Delta\varepsilon_{AI}} \gg 1, \tag{S5}$$

$$\gamma_1 e^{-\beta\Delta\varepsilon_{AI}} \gg 1, \tag{S6}$$

$$\gamma_2 e^{-\beta\Delta\varepsilon_{AI}} \gg 1, \tag{S7}$$

$$\gamma_1\gamma_2 e^{-\beta\Delta\varepsilon_{AI}} \ll 1. \tag{S8}$$

Combining eqs S6-S8, we obtain the condition for an AND gate, namely,

$$\frac{1}{\gamma_1}, \frac{1}{\gamma_2} \ll e^{-\beta\Delta\varepsilon_{AI}} \ll \frac{1}{\gamma_1\gamma_2}. \tag{S9}$$

Note, that the outer inequalities imply

$$\gamma_1, \gamma_2 \ll 1, \tag{S10}$$

meaning that both ligands bind more tightly to the protein in the active than the inactive state.

A.2 OR Gate

For p_{active} to represent an OR gate across ligand concentration space, it must satisfy $p_{0,0} \approx 0$, $p_{0,\infty} \approx 1$, $p_{\infty,0} \approx 1$ and $p_{\infty,\infty} \approx 1$. This requires that the parameters obey

$$e^{-\beta\Delta\varepsilon_{AI}} \gg 1, \tag{S11}$$

$$\gamma_1 e^{-\beta\Delta\varepsilon_{AI}} \ll 1, \tag{S12}$$

$$\gamma_2 e^{-\beta\Delta\varepsilon_{AI}} \ll 1, \tag{S13}$$

$$\gamma_1\gamma_2 e^{-\beta\Delta\varepsilon_{AI}} \ll 1. \tag{S14}$$

Combining eqs S11-S13, we obtain a constraint on the free energy difference,

$$1 \ll e^{-\beta\Delta\varepsilon_{AI}} \ll \frac{1}{\gamma_1}, \frac{1}{\gamma_2}. \tag{S15}$$

As with the AND gate, the outer inequalities imply that the ligands prefer binding to the protein in the active state,

$$\gamma_1, \gamma_2 \ll 1. \tag{S16}$$

A.3 NAND and NOR Gates

Because the NAND and NOR gates are the logical complements of AND and OR gates, respectively, the parameter constraints under which they are realized are the opposites of

those for AND and OR gates. Hence, the conditions for a NAND gate are given by

$$\frac{1}{\gamma_1\gamma_2} \ll \mathrm{e}^{-\beta\Delta\varepsilon_{\mathrm{AI}}} \ll \frac{1}{\gamma_1}, \frac{1}{\gamma_2} \tag{S17}$$

while the conditions for NOR gates are

$$\frac{1}{\gamma_1}, \frac{1}{\gamma_2} \ll \mathrm{e}^{-\beta\Delta\varepsilon_{\mathrm{AI}}} \ll 1. \tag{S18}$$

We note that in both cases, the outer inequalities imply that both ligands bind more tightly to the protein in the inactive state than in the active state, $\gamma_1, \gamma_2 \gg 1$.

The symmetry between AND/OR and NAND/NOR gates also implies a simple relation between their quality metrics, namely, $\mathrm{Q}_{\mathrm{AND/OR}}\left(\gamma_1, \gamma_2, \Delta\varepsilon_{\mathrm{AI}}\right) = \mathrm{Q}_{\mathrm{NAND/NOR}}\left(\frac{1}{\gamma_1}, \frac{1}{\gamma_2}, -\Delta\varepsilon_{\mathrm{AI}}\right)$. Here we provide a proof for the AND gate and invite the reader to do the same for the OR gate. From eq 2, the quality metrics for the AND and NAND gates can be written as

$$\begin{aligned}
\mathrm{Q}_{\mathrm{AND}}(\gamma_1, \gamma_2, \omega) &= (1 - \mathrm{p}_{0,0})(1 - \mathrm{p}_{\infty,0})(1 - \mathrm{p}_{0,\infty})\mathrm{p}_{\infty,\infty} \\
&= \left(1 - \frac{1}{1+\omega}\right)\left(1 - \frac{1}{1+\gamma_1\omega}\right)\left(1 - \frac{1}{1+\gamma_2\omega}\right)\left(\frac{1}{1+\gamma_1\gamma_2\omega}\right) \\
&= \frac{\gamma_1\gamma_2\omega^3}{(1+\omega)(1+\gamma_1\omega)(1+\gamma_2\omega)(1+\gamma_1\gamma_2\omega)}, \qquad \text{(S19)} \\
\mathrm{Q}_{\mathrm{NAND}}(\gamma_1, \gamma_2, \omega) &= \mathrm{p}_{0,0}\mathrm{p}_{\infty,0}\mathrm{p}_{0,\infty}(1 - \mathrm{p}_{\infty,\infty}) \\
&= \left(\frac{1}{1+\omega}\right)\left(\frac{1}{1+\gamma_1\omega}\right)\left(\frac{1}{1+\gamma_2\omega}\right)\left(1 - \frac{1}{1+\gamma_1\gamma_2\omega}\right) \\
&= \frac{\gamma_1\gamma_2\omega}{(1+\omega)(1+\gamma_1\omega)(1+\gamma_2\omega)(1+\gamma_1\gamma_2\omega)}, \qquad \text{(S20)}
\end{aligned}$$

where we introduced $\omega = \mathrm{e}^{-\beta\Delta\varepsilon_{\mathrm{AI}}}$. Substituting $\gamma_1 \to \gamma_1^{-1}, \gamma_2 \to \gamma_2^{-1}, \omega \to \omega^{-1}$ (equivalent to $\Delta\varepsilon_{\mathrm{AI}} \to -\Delta\varepsilon_{\mathrm{AI}}$) in eq S20, we obtain

$$\begin{aligned}
\mathrm{Q}_{\mathrm{NAND}}(\gamma_1^{-1}, \gamma_2^{-1}, \omega^{-1}) &= \frac{\gamma_1^{-1}\gamma_2^{-1}\omega^{-1}}{(1+\omega^{-1})(1+\gamma_1^{-1}\omega^{-1})(1+\gamma_2^{-1}\omega^{-1})(1+\gamma_1^{-1}\gamma_2^{-1}\omega^{-1})} \times \frac{\gamma_1^2\gamma_2^2\omega^4}{\gamma_1^2\gamma_2^2\omega^4} \\
&= \frac{\gamma_1\gamma_2\omega^3}{(1+\omega)(1+\gamma_1\omega)(1+\gamma_2\omega)(1+\gamma_1\gamma_2\omega)} \\
&\equiv \mathrm{Q}_{\mathrm{AND}}(\gamma_1, \gamma_2, \omega). \qquad \text{(S21)}
\end{aligned}$$

A.4 XOR and XNOR Gates

Here, we show that the XOR gate (and by symmetry the XNOR gate) are not achievable with the form of $\mathrm{p}_{\mathrm{active}}$ given in eq 1. An XOR gate satisfies $\mathrm{p}_{0,0} \approx 0$, $\mathrm{p}_{0,\infty} \approx 1$, $\mathrm{p}_{\infty,0} \approx 1$ and $\mathrm{p}_{\infty,\infty} \approx 0$ which necessitates the parameter conditions

$$\mathrm{e}^{-\beta\Delta\varepsilon_{\mathrm{AI}}} \gg 1, \tag{S22}$$

$$\gamma_1 e^{-\beta\Delta\varepsilon_{AI}} \ll 1, \tag{S23}$$

$$\gamma_2 e^{-\beta\Delta\varepsilon_{AI}} \ll 1, \tag{S24}$$

$$\gamma_1\gamma_2 e^{-\beta\Delta\varepsilon_{AI}} \gg 1. \tag{S25}$$

However, these conditions cannot all be satisfied, as the left-hand side of eq S25 can be written in terms of the left-hand sides of eqs S22-S24,

$$\gamma_1\gamma_2 e^{-\beta\Delta\varepsilon_{AI}} = \frac{\left(\gamma_1 e^{-\beta\Delta\varepsilon_{AI}}\right)\left(\gamma_2 e^{-\beta\Delta\varepsilon_{AI}}\right)}{e^{-\beta\Delta\varepsilon_{AI}}} \ll 1, \tag{S26}$$

contradicting eq S25.

The XOR gate could be realized if an explicit cooperativity energy $\varepsilon_{A,coop}$ is added when both ligands are bound in the active state and $\varepsilon_{I,coop}$ when both are bound in the inactive state. These cooperative interactions modify eq 1 to the form

$$p_{active}([L_1],[L_2]) = \frac{1 + \frac{[L_1]}{K_{A,1}} + \frac{[L_2]}{K_{A,2}} + \frac{[L_1]}{K_{A,1}}\frac{[L_2]}{K_{A,2}} e^{-\beta\varepsilon_{A,coop}}}{1 + \frac{[L_1]}{K_{A,1}} + \frac{[L_2]}{K_{A,2}} + \frac{[L_1]}{K_{A,1}}\frac{[L_2]}{K_{A,2}} e^{-\beta\varepsilon_{A,coop}} + e^{-\beta\Delta\varepsilon_{AI}}\left(1 + \frac{[L_1]}{K_{I,1}} + \frac{[L_2]}{K_{I,2}} + \frac{[L_1]}{K_{I,1}}\frac{[L_2]}{K_{I,2}} e^{-\beta\varepsilon_{I,coop}}\right)}. \tag{S27}$$

Figure S2 demonstrates that the same parameter values from Figure 3B together with the (unfavorable) cooperativity energy $\varepsilon_{A,coop} = 15\,k_BT$ and $\varepsilon_{I,coop} = 0$ can create an XOR gate.

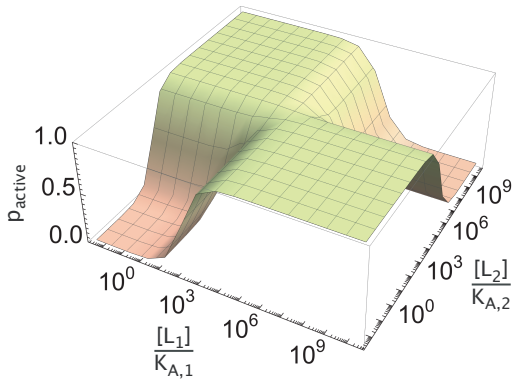

Figure S2. An XOR gate can be achieved by adding cooperativity. The activity profile defined in eq S27 for the parameter values from Figure 3B, along with the cooperativity energies $\varepsilon_{A,coop} = 15\,k_BT$ and $\varepsilon_{I,coop} = 0$, give rise to an XOR response.

B The General Two-Ligand Response: Transitioning Between OFF and ON States

In the preceding section, we have been solely concerned with the behavior of the MWC molecule in the limits of ligand concentration ($[L_i] = 0$ and $[L_i] \to \infty$), and have ignored the details about the transition from ON to OFF (e.g., its shape and steepness) and also the possibility of $p_{active} \neq 0$ or 1. In this section, we examine and derive in greater detail some of the additional response behaviors that are possible for an MWC molecule regulated with $N = 2$ ligands when the locations of transitions between limit responses are taken into account.

To examine the transitions between p_{active} levels, we derive expressions for the concentrations at which transitions are at their midpoint. Since p_{active} is a function of two different ligand concentrations, $[L_1]$ and $[L_2]$, we define two different midpoint concentrations of ligand L_i: one in the absence of ligand L_j, $[L_i^*]_{[L_j]\to 0}$, and another when L_j is saturating, $[L_i^*]_{[L_j]\to\infty}$. In particular, $[L_i^*]_{[L_j]\to 0}$ is defined such that

$$p_{active}\left([L_i^*]_{[L_j]\to 0}, [L_j] = 0\right) = \frac{p_{active}\left([L_i] = 0, [L_j] = 0\right) + p_{active}\left([L_i] \to \infty, [L_j] = 0\right)}{2}, \quad \text{(S28)}$$

i.e., the concentration of ligand i where p_{active} is equal to the mean of the two p_{active} limit values being transitioned between. If we evaluate the left hand side of eq S28 with $i = 1$ and $j = 2$ using eq 1, and the right hand side using the limits from Figure 3(A), we obtain

$$\frac{\left(1 + \frac{[L_1^*]_{[L_2]\to 0}}{K_{A,1}}\right)}{\left(1 + \frac{[L_1^*]_{[L_2]\to 0}}{K_{A,1}}\right) + e^{-\beta\Delta\varepsilon_{AI}}\left(1 + \frac{[L_1^*]_{[L_2]\to 0}}{K_{I,1}}\right)} = \frac{1}{2}\left(\frac{1}{1 + e^{-\beta\Delta\varepsilon_{AI}}} + \frac{1}{1 + \gamma_1 e^{-\beta\Delta\varepsilon_{AI}}}\right). \quad \text{(S29)}$$

Introducing $\gamma_1 = K_{A,1}/K_{I,1}$, we can solve for $[L_1^*]_{[L_2]\to 0}$ to find

$$\frac{[L_1^*]_{[L_2]\to 0}}{K_{A,1}} = \frac{1 + e^{-\beta\Delta\varepsilon_{AI}}}{1 + \gamma_1 e^{-\beta\Delta\varepsilon_{AI}}}. \quad \text{(S30)}$$

Eq S30 can be rewritten for $[L_2^*]_{[L_1]\to 0}$ by merely interchanging all ligand and parameter indices, i.e., $1 \leftrightarrow 2$.

The midpoint concentration when one ligand is saturating can be derived similarly. Specifically, to find an expression for $[L_i^*]_{[L_j]\to\infty}$ we can re-write S28 using eq 1 in the case that $[L_j] \to \infty$ with $i = 1$ and $j = 2$, resulting in

$$\frac{\left(1 + \frac{[L_1^*]_{[L_2]\to\infty}}{K_{A,1}}\right)}{\left(1 + \frac{[L_1^*]_{[L_2]\to\infty}}{K_{A,1}}\right) + \gamma_2 e^{-\beta\Delta\varepsilon_{AI}}\left(1 + \frac{[L_1^*]_{[L_2]\to\infty}}{K_{I,1}}\right)} = \frac{1}{2}\left(\frac{1}{1 + \gamma_2 e^{-\beta\Delta\varepsilon_{AI}}} + \frac{1}{1 + \gamma_1\gamma_2 e^{-\beta\Delta\varepsilon_{AI}}}\right). \quad \text{(S31)}$$

Eq S31 can be solved for $[L_1^*]_{[L_2]\to\infty}$ to produce,

$$\frac{[L_1^*]_{[L_2]\to\infty}}{K_{A,1}} = \frac{1+\gamma_2\, e^{-\beta\Delta\varepsilon_{AI}}}{1+\gamma_1\gamma_2\, e^{-\beta\Delta\varepsilon_{AI}}}. \tag{S32}$$

Again, the symmetric expression for $[L_2^*]_{[L_1]\to\infty}$ is found by swapping ligand and parameter indices, $1\leftrightarrow 2$.

Using this approach to define concentration transition zones can be used to produce additional MWC behaviors, including the ratiometric response in the BMP pathway recently analyzed by Antebi *et al.*,[8] which was briefly discussed earlier. Specifically, this response can be approximated by choosing parameter values that satisfy two desired limits, $p_{\infty,0} \approx 0$ ($\gamma_1\, e^{-\beta\Delta\varepsilon_{AI}} \gg 1$) and $p_{0,\infty} \approx 1$ ($\gamma_2\, e^{-\beta\Delta\varepsilon_{AI}} \ll 1$), as well as produce a large transition region sensitive to both ligands, i.e., the ratio in eq 7, $\frac{[L_i^*]_{[L_j]\to\infty}}{[L_i^*]_{[L_j]\to 0}}$ is far from 1. One way to satisfy these conditions is to set $K_{I,2} \gg K_{A,1} = K_{A,2} \gg K_{I,1}$ and $\Delta\varepsilon_{AI} = 0$ in eq 1. Notice that with these parameter choices and provided the ligand concentrations satisfy

$$\begin{aligned} \frac{[L_1]}{K_{A,1}}, \frac{[L_2]}{K_{I,2}} &\ll 1, \\ \frac{[L_1]}{K_{I,1}}, \frac{[L_2]}{K_{A,2}} &\gg 1, \end{aligned} \tag{S33}$$

the probability that the protein is active reduces to

$$p_{\text{active}}\left([L_1],[L_2]\right) \approx \frac{\frac{[L_2]}{K_{A,2}}}{\frac{[L_2]}{K_{A,2}} + \frac{[L_1]}{K_{I,1}}}. \tag{S34}$$

Hence, only the ratio of $[L_1]$ and $[L_2]$ matters, as shown in Figure 4B where eq S33 is satisfied provided that $10^{-4} \lesssim \frac{[L_1]}{K_{A,1}} \lesssim 10^0 \lesssim \frac{[L_2]}{K_{A,2}} \lesssim 10^4$.

Additionally, we consider the remaining three types of input-output computations shown by Antebi *et al.* to exist in the BMP pathway which they called the additive, imbalance, and balance responses.[8] The additive response (which responds more to larger input concentrations) is an OR gate which we showed is possible in Figure 3B. The imbalance response (which responds maximally to extreme ratios of the two input ligands) is similar to an XOR behavior which, as discussed in Appendix A.4, is only achievable with an explicit cooperativity energy.

The balance response is defined as

$$p_{\text{active}}^{\text{balance}} = \begin{cases} 1 & [L_1] \approx [L_2] \\ 0 & [L_1] \not\approx [L_2] \end{cases} \tag{S35}$$

so that the protein is only ON when both ligands are present in the same amount as shown in Figure S3A. Such behavior is not possible within the MWC model because starting from any point $\overline{[L_1]} = \overline{[L_2]}$, p_{active} in eq 1 must either monotonically increase or monotonically decrease with $[L_1]$ (depending on γ_1), whereas eq S35 requires that p_{active} must decrease for

both $[L_1] > \overline{[L_1]}$ and $[L_1] < \overline{[L_1]}$ (with similar contradictory statements for $[L_2]$). The closest behavior achievable by the MWC model is to zoom into the transition region of an XNOR gate as shown in Figure S3B. As we zoom out of the concentration ranges shown, the four square regions of the plot will continue to expand as squares and the behavior will no longer approximate the ideal balance response.

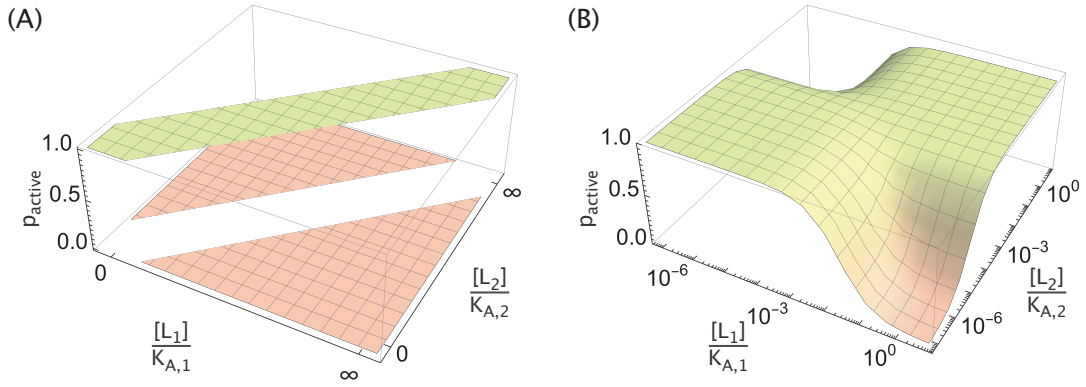

Figure S3. Balance response behavior approximated by the MWC model. (A) The ideal balance response from the BMP pathway and (B) the closest behavior that an MWC molecule can exhibit using the complementary parameters from Figure S2 ($K_{A,i} = 1.5 \times 10^{-4}\,M$, $K_{I,i} = 2.5 \times 10^{-8}\,M$, $\Delta\varepsilon_{AI} = 5\,k_BT$, $\varepsilon_{A,coop} = -15\,k_BT$ and $\varepsilon_{I,coop} = 0$).

C Logic Switching by Tuning the Number of Ligand Binding Sites

In this section, we show how an MWC molecule whose activity is given by eq 9 can switch between exhibiting AND↔OR or NAND↔NOR behaviors by tuning the number of binding sites. To begin, we define the probability p_{active} that the molecule is active in the case when the i^{th} ligand has n_i binding sites, namely,

$$p_{0,0} = p_{active}([L_1] \to 0, [L_2] \to 0) = \frac{1}{1 + e^{-\beta\Delta\varepsilon_{AI}}}, \tag{S36}$$

$$p_{\infty,0} = p_{active}([L_1] \to \infty, [L_2] \to 0) = \frac{1}{1 + \gamma_1^{n_1} e^{-\beta\Delta\varepsilon_{AI}}}, \tag{S37}$$

$$p_{0,\infty} = p_{active}([L_1] \to 0, [L_2] \to \infty) = \frac{1}{1 + \gamma_2^{n_2} e^{-\beta\Delta\varepsilon_{AI}}}, \tag{S38}$$

$$p_{\infty,\infty} = p_{active}([L_1] \to \infty, [L_2] \to \infty) = \frac{1}{1 + \gamma_1^{n_1}\gamma_2^{n_2} e^{-\beta\Delta\varepsilon_{AI}}}. \tag{S39}$$

Note that the only effect of having an arbitrary number of ligand binding sites (as opposed to $n_i = 1$ as in Appendix A) is that the ratio of dissociation constants always appears raised to the number of binding sites, $\gamma_i^{n_i}$. Hence, the parameter conditions derived for AND and OR behaviors for $n_i = 1$ can be used in the case of general n_i by substituting $\gamma_i \to \gamma_i^{n_i}$.

Now, suppose a molecule with $N = 2$ ligands and with n_1' and n_2' binding sites for ligands 1 and 2 represents an AND gate, while this same molecule with n_1 and n_2 binding sites serves as an OR gate, as in Figure 5B with $n_1' = n_2' = 1$ and $n_1 = n_2 = 4$. From Figure 3B, the conditions in the former case (AND gate) are

$$\frac{1}{\gamma_1^{n_1'}}, \frac{1}{\gamma_2^{n_2'}} \ll e^{-\beta\Delta\varepsilon_{AI}} \ll \frac{1}{\gamma_1^{n_1'}\gamma_2^{n_2'}}, \tag{S40}$$

while the conditions in the latter case (OR gate) are

$$1 \ll e^{-\beta\Delta\varepsilon_{AI}} \ll \frac{1}{\gamma_1^{n_1}}, \frac{1}{\gamma_2^{n_2}}. \tag{S41}$$

Combining these conditions, we find that the requirements for the AND↔OR switching are given by

$$\frac{1}{\gamma_1^{n_1'}}, \frac{1}{\gamma_2^{n_2'}} \ll e^{-\beta\Delta\varepsilon_{AI}} \ll \frac{1}{\gamma_1^{n_1}}, \frac{1}{\gamma_2^{n_2}}, \frac{1}{\gamma_1^{n_1'}\gamma_2^{n_2'}}, \tag{S42}$$

where we have used the fact that the outer inequalities imply $\gamma_1^{n_1'}, \gamma_2^{n_2'} \ll 1$ (so that $1 \ll \frac{1}{\gamma_1^{n_1'}}, \frac{1}{\gamma_2^{n_2'}}$). In the limit $n_1' = n_2' = 1$, eq S42 reduces to the condition shown in Figure 5A.

Lastly, we note that since NAND is the complement of AND while NOR is the complement of OR, the class switching requirements in S42 become the requirements to change from NAND↔NOR behavior when $\gamma_i \to \frac{1}{\gamma_i}$ and $\Delta\varepsilon_{AI} \to -\Delta\varepsilon_{AI}$.

D Combinatorial Control with Three Regulatory Ligands

In this section, we first present the methodology used to identify the functionally unique and MWC-compatible 3-ligand logic gates. We then use the full list of admissible gates to find all possible logic switches that can be induced by increasing the concentration of a third ligand. We finish the section by deriving the parameter conditions required for achieving the logic switches AND→OR and AND→YES$_1$ shown in Figure 7D.

D.1 Functionally Unique MWC Gates

To identify the set of functionally unique MWC gates, we first iterate over the 256 possible responses and eliminate those redundant ones that can be obtained by shuffling the ligand labels of already selected gates. The Python implementation of this procedure that leaves 80 functionally unique gates can be found in the supplementary Jupyter Notebook 1.

Having singled out the functionally unique responses, we proceed to identify those that are admissible in the MWC framework. To that end, we first write the analytic forms for the probability of the protein being active (p_{active}) at eight different ligand concentration limits (Figure S4A). Since the functional form in all cases is $p_{active} = (1 + w_{I/A})^{-1}$, where $w_{I/A}$ is the total weight of the inactive states divided by the total weight of the active states in the appropriate limit (as seen in Figure 3A), a Boolean response ($p_{active} \approx 0$ or 1) can only be achieved when $w_{I/A} \gg 1$ or $w_{I/A} \ll 1$, respectively. Hence, the values of $w_{I/A}$ at the eight different limits of ligand concentration will determine the full logic response of the protein.

Note that since cooperative interactions between ligands are absent in the MWC framework, the eight different $w_{I/A}$ expressions depend on only four independent MWC parameters, namely, $\{\Delta\varepsilon_{AI}, \gamma_1, \gamma_2, \gamma_3\}$. Therefore, only four of the eight limiting $w_{I/A}$ values can be independently tuned, and any $w_{I/A}$ limit can be expressed as a function of four different and independent $w_{I/A}$ limits, resulting in a constraint condition. Since each $w_{I/A}$ is a product of some γ_i's and $e^{-\beta\Delta\varepsilon_{AI}}$ (Figure S4A), we look for constraint conditions that have a multiplicative form, namely,

$$w_{s^*} = \prod_{i=1}^{4} w_{s_n}^{\alpha_n}, \tag{S43}$$

where w_{s^*} is the target limit, $s_n \neq s^* (1 \leq n \leq 4)$ are the labels of four different limits and α_n are real coefficients. Searching over all conditions of such form (see the supplementary Jupyter Notebook 2 for details), we identify a total of eight functionally unique constraints,

$$w_{ij} \times w_0 = w_i \times w_j, \tag{S44}$$
$$w_{123} \times w_j = w_{ij} \times w_{jk}, \tag{S45}$$
$$w_{ij} \times w_k = w_{ik} \times w_j, \tag{S46}$$
$$w_{123} \times w_0 = w_{ij} \times w_k, \tag{S47}$$
$$w_{ij} \times w_k^2 = w_0 \times w_{ik} \times w_{jk}, \tag{S48}$$
$$w_{123} \times w_0^2 = w_1 \times w_2 \times w_3, \tag{S49}$$
$$w_{123}^2 \times w_0 = w_{12} \times w_{13} \times w_{23}, \tag{S50}$$

$$w_{123} \times w_i \times w_j = w_{ij}^2 \times w_k, \tag{S51}$$

where $1 \leq i, j, k \leq 3$.

Further searching for a minimum set of constraints that can account for all gates incompatible with the MWC framework, we identify the constraints in eqs S44-S47 as the necessary and sufficient ones (see the supplementary Jupyter Notebook 2). Graphical representations of these four constraints on a cubic diagram are shown in Figure S4B. Note that these conditions are all of the form

$$w_{s_1} w_{s_2} = w_{s_3} w_{s_4}, \tag{S52}$$

where s_i are labels corresponding to different ligand concentration limits. Logic responses where $w_{s_1}, w_{s_2} \ll 1 \, (\gg 1)$ while $w_{s_3}, w_{s_4} \gg 1 \, (\ll 1)$ cannot be achieved, since they contradict the constraint condition. Conditions 1 and 2 in Figure S4B, for example, demonstrate that XOR and XNOR gates cannot be realized by any two ligands in the absence (condition 1) or presence (condition 2) of a third ligand - a result expected from the 2-ligand analysis done earlier. On the other hand, conditions 3 and 4 are specific to the 3-ligand response.

Checking the 80 functionally unique gates against the four constraints in Figure S4B, we obtain a set of 34 functionally unique and MWC-compatible gates, 17 of which are shown in Figure S5A while the other half are their logical complements (i.e. ON↔OFF swapping is performed for each of the cube elements).

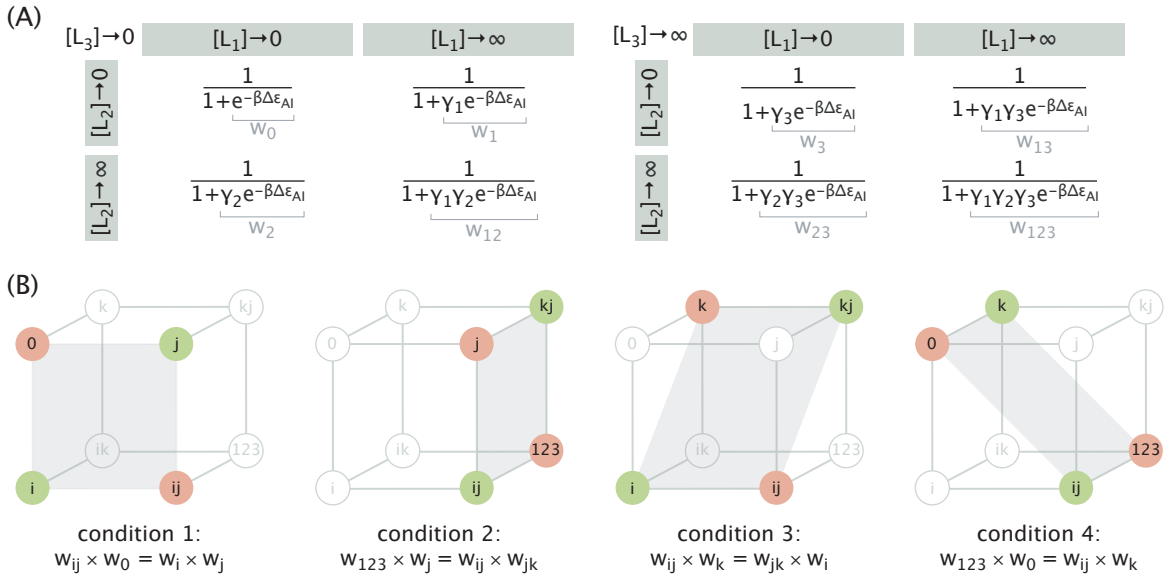

Figure S4. Three-ligand logic gates that are incompatible with the MWC framework. (A) Probability that the protein is active in the 8 different ligand concentration limits. The total weight of the inactive states relative to the active states is indicated in gray for all limits. (B) Cubic diagrams of logic responses that are incompatible with the MWC framework, along with the constraint equations used to obtain them. The limits relevant to the constraint conditions are shown in color, and a transparent gray plane containing these relevant limits is added for clarity. In all four diagrams $1 \leq i, j, k \leq 3$.

D.2 Logic Switching

Here we describe how the table of all possible logic switches inducible by a third ligand (Figure 6D) can be obtained from the list of MWC-compatible 3-ligand gates (Figure S5), and also derive the parameter conditions for AND→OR and AND→YES_1 logic switches.

As illustrated in Figure 6C, logic switching can be achieved by increasing the concentration of any of the three ligands. Following the same procedure, we iterate over the list of gates shown in Figure S5A and for each of them identify the set of possible logic switches. The set of all logic switches present in Figure S5A together constitute the entries of the table in Figure 6D. Note that if a gate is compatible with the MWC framework, then its logical complement is also compatible, and therefore, the possibility of switching between two gates, Gate 1 → Gate 2, implies the possibility of switching between their logical complements, NOT (Gate 1) → NOT (Gate 2).

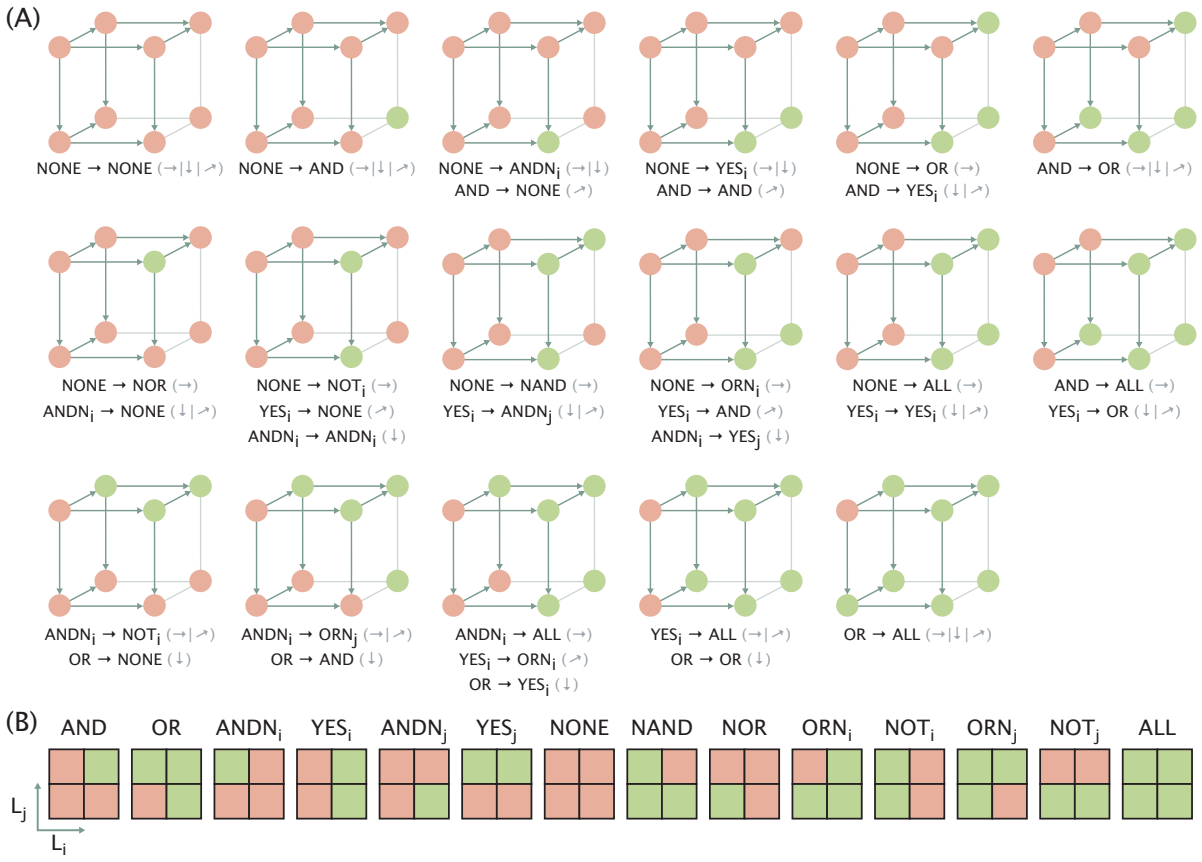

Figure S5. Functionally unique 3-ligand MWC gates and possible schemes of logic switching. (A) List of functionally unique 3-ligand MWC gates that have an inactive base state (in the absence of ligands). The set of logic switches that can be achieved by increasing the concentration of one of the ligands is listed on the bottom of each gate, with the gray arrows indicating the corresponding directions of increasing ligand concentration. Transitions with swapped labels (i ↔ j) are also possible and are not listed. Arrows corresponding to the ligand axes on different faces of the cube are included to assist the derivation of possible logic switches. (B) Schematics of 2-ligand gates adapted from Figure 6D for convenience.

Now, we show how an MWC protein can exhibit the switching behaviors in Figure 7B,D (AND→OR and AND→YES$_1$) by saturating the concentration of the third ligand. We first consider the behavior of the protein in the absence of the third ligand ($[L_3] = 0$, with p_{active} limits given in Figure S4A, left) and then consider how the protein acts at the saturating concentration of the third ligand ($[L_3] \to \infty$, with p_{active} limits given in Figure S4A, right). With $[L_3] = 0$, the protein ignores the third ligand and behaves identically to a protein with $N = 2$ ligands. In the limit $[L_3] \to \infty$, however, the protein behaves as if it only has two ligands with an altered free energy difference $\Delta\varepsilon'_{AI}$ between the active and inactive states given by

$$\Delta\varepsilon'_{AI} = \Delta\varepsilon_{AI} - k_B T \log \gamma_3. \tag{S53}$$

Suppose that a protein acts as an AND gate when $[L_3] = 0$ and transitions into an OR gate when $[L_3] \to \infty$, as in Figure 7B. From Figure 3B, the MWC parameters must satisfy

$$\frac{1}{\gamma_1}, \frac{1}{\gamma_2} \ll e^{-\beta\Delta\varepsilon_{AI}} \ll \frac{1}{\gamma_1\gamma_2} \tag{S54}$$

in the absence of L_3 (AND behavior) and

$$1 \ll e^{-\beta\Delta\varepsilon'_{AI}} \ll \frac{1}{\gamma_1}, \frac{1}{\gamma_2} \tag{S55}$$

when $[L_3]$ is saturating (OR behavior). Using eqs S53, we can rewrite the condition S55 as

$$\frac{1}{\gamma_3} \ll e^{-\beta\Delta\varepsilon_{AI}} \ll \frac{1}{\gamma_1\gamma_3}, \frac{1}{\gamma_2\gamma_3}. \tag{S56}$$

Combining eq S54 and eq S56, we find the second condition reported in Figure 7A, namely,

$$\frac{1}{\gamma_1}, \frac{1}{\gamma_2}, \frac{1}{\gamma_3} \ll e^{-\beta\Delta\varepsilon_{AI}} \ll \frac{1}{\gamma_1\gamma_2}, \frac{1}{\gamma_1\gamma_3}, \frac{1}{\gamma_2\gamma_3}. \tag{S57}$$

The first condition in Figure 7A is then obtained by using the outer inequalities, that is,

$$\frac{1}{\gamma_k} \ll \frac{1}{\gamma_i\gamma_j} \Rightarrow \gamma_i\gamma_j \ll \gamma_k \quad \text{and} \tag{S58}$$

$$\frac{1}{\gamma_i} \ll \frac{1}{\gamma_i\gamma_k} \Rightarrow \gamma_k \ll 1. \tag{S59}$$

Lastly, we derive the parameter conditions needed to achieve an AND→YES$_1$ switching by saturating the third ligand. Conditions for the AND behavior in the absence of the third ligand are already known (eq S54). To achieve a YES$_1$ gate, p_{active} at $[L_3] \to \infty$ needs to meet the following limits:

$$p_{0,0,\infty} = \frac{1}{1 + \gamma_3 e^{-\beta\Delta\varepsilon_{AI}}} \approx 0, \tag{S60}$$

$$p_{0,\infty,\infty} = \frac{1}{1+\gamma_2\gamma_3 e^{-\beta\Delta\varepsilon_{AI}}} \approx 0, \tag{S61}$$

$$p_{\infty,0,\infty} = \frac{1}{1+\gamma_1\gamma_3 e^{-\beta\Delta\varepsilon_{AI}}} \approx 1, \tag{S62}$$

$$p_{\infty,\infty,\infty} = \frac{1}{1+\gamma_1\gamma_2\gamma_3 e^{-\beta\Delta\varepsilon_{AI}}} \approx 1. \tag{S63}$$

These limits suggest constraints on $\Delta\varepsilon_{AI}$, which, combined with eq S54, result in

$$\frac{1}{\gamma_1}, \frac{1}{\gamma_2}, \frac{1}{\gamma_3}, \frac{1}{\gamma_2\gamma_3} \ll e^{-\beta\Delta\varepsilon_{AI}} \ll \frac{1}{\gamma_1\gamma_2}, \frac{1}{\gamma_1\gamma_3}, \frac{1}{\gamma_2\gamma_3}, \frac{1}{\gamma_1\gamma_2\gamma_3}. \tag{S64}$$

The outer inequalities, in turn, suggest conditions for the γ parameters, namely,

$$\frac{1}{\gamma_i} \ll \frac{1}{\gamma_i\gamma_k} \Rightarrow \gamma_k \ll 1, \tag{S65}$$

$$\frac{1}{\gamma_2\gamma_3} \ll \frac{1}{\gamma_1\gamma_2} \Rightarrow \gamma_1 \ll \gamma_2, \tag{S66}$$

$$\frac{1}{\gamma_2\gamma_3} \ll \frac{1}{\gamma_1\gamma_3} \Rightarrow \gamma_1 \ll \gamma_3. \tag{S67}$$

Accounting for these additional constraints, eq S64 simplifies into

$$\frac{1}{\gamma_1}, \frac{1}{\gamma_2\gamma_3} \ll e^{-\beta\Delta\varepsilon_{AI}} \ll \frac{1}{\gamma_1\gamma_2}, \frac{1}{\gamma_1\gamma_3}, \tag{S68}$$

as shown in Figure 7C.